

# Magnetization-Transfer NMR Analysis of Aqueous Poly(vinyl alcohol) Gels: Effect of Hydrolysis and Storage Temperature on Network Formation

Lori E. Stephans and Natalie Foster\*

Department of Chemistry, Lehigh University, Bethlehem, Pennsylvania 18015

Received September 26, 1997; Revised Manuscript Received January 6, 1998

**ABSTRACT:** The technique of magnetization-transfer nuclear magnetic resonance (MT-NMR) was used to probe the effects of concentration, degree of hydrolysis, and storage temperature on the formation of a network in aqueous solutions and gels of atactic poly(vinyl alcohol) (PVA). The average degree of polymerization of the samples was 1250–1300, and the degrees of hydrolysis of the polymers were 99.5, 98.5, 97.4, and 87.6 mol %. The area of MT profiles and hence the extent of network formation increases nonlinearly with increasing concentration for all PVA samples evaluated, with more extensive network associated with higher polymer concentrations. Network formation is minimal at all concentrations for PVA that is 87.6% hydrolyzed (12.4% residual acetate); the critical concentration of residual acetate groups necessary to disrupt the polymer–polymer hydrogen bonding responsible for forming the network is in the range of 3%. The development of the network proceeds over a period of as long as 18 weeks and is highly sensitive to storage temperature. An analysis of the Gaussian and Lorentzian components of MT profiles indicates that a sample whose profile area is greater than 50% Gaussian may be considered a gel from the point of view of NMR.

## Introduction

Poly(vinyl alcohol) (PVA) is the largest volume, synthetic, water-soluble polymer manufactured in the United States and Japan.<sup>1–3</sup> PVA, prepared by the hydrolysis of poly(vinyl acetate), is commercially available with a broad range of physical properties that depend on the degree of hydrolysis and extent of polymerization. These diverse physical properties make numerous applications possible, including textile and paper sizing, adhesives, fibers, and films.<sup>4</sup> The degree of hydrolysis, which represents the percent conversion of acetate groups to hydroxyl groups, significantly affects PVA solubility and the viscosity of its aqueous solutions.

Residual acetate groups in partially hydrolyzed PVA improve water solubility by disrupting polymer–polymer interchain and intrachain hydrogen bonding between hydroxyl groups and thereby promoting polymer–solvent interactions. The larger number of hydroxyl groups in fully hydrolyzed PVA decreases water solubility by promoting physical entanglements in solution through the preferential formation of polymer–polymer interchain and intrachain hydrogen bonds. Variability in the extent and strength of these physical entanglements causes complex behavior in PVA solutions and gels and dictates the physical properties and quality of finished products. The evolution of the network is strongly affected by the manner in which the initial dissolution of the polymer is carried out as well as by the storage conditions. As a result, considerable interest has focused on understanding the basic principles that govern the behavior of solutions and gels at a molecular level from the point of view of both polymer and solvent.<sup>5–9</sup>

The physical process of aging in PVA gels is characterized by increasing viscosity and loss of fluidity. The rate and extent to which aging proceeds in the aqueous medium are primarily affected by the molecular weight, degree of hydrolysis, tacticity, and concentration of the polymer. Molecular processes such as network formation, gelation, and phase separation collectively cause physical aging. Consequently, PVA research has focused on the elucidation of the physical structure of the network in the aqueous medium and in mixed solvents.<sup>10–12</sup>

Physical aging in dilute aqueous solutions of PVA has been probed by wide-angle X-ray scattering,<sup>13</sup> dynamic light scattering,<sup>14</sup> small-angle neutron scattering,<sup>15</sup> and rheology.<sup>16–18</sup> A wealth of information concerning the effects of the physical properties of PVA on film and fiber formation has been provided by studies involving differential scanning calorimetry, infrared spectroscopy, and mechanical measurements.<sup>4,19–21</sup> The majority of these techniques: (i) require the sample to be a film or in dilute solution, (ii) are not adaptable to concentrated solutions or gels, (iii) provide static measurements that are complicated by gelation, and (iv) have only involved the analysis of fully hydrolyzed PVA. This investigation uses nuclear magnetic resonance (NMR) techniques, specifically magnetization transfer (MT), to nondestructively probe the effects of the degree of hydrolysis and the storage temperature on network formation in aqueous PVA gels over a broad range of concentrations without limitations on the physical state of the sample.

## Experimental Methods and Materials

**Materials.** Atactic poly(vinyl alcohol) with an average degree of polymerization (dp) of 1250–1300 and degrees of hydrolysis of 99.5 for PVA-A, 98.5 for PVA-B, 97.4 for PVA-C, and 87.6 for PVA-D (mole percent hydrolysis) was supplied by Air Products and Chemicals, Inc., Allentown, PA. Poly(ethylene oxide) (PEO) with a viscosity-average molecular weight of 100 000 was obtained from Aldrich, Milwaukee, WI.

\* To whom correspondence should be addressed at Department of Chemistry, 6 East Packer Avenue, Lehigh University, Bethlehem, PA 18015. E-mail: nf00@lehigh.edu. Telephone: 610-758-3646. Fax: 610-758-3461.

Distilled water (conductivity:  $4 \text{ m}\Omega^{-1}/\text{cm}$ ; pH 5.4) was used to prepare all samples.

**Methods.** PVA and room-temperature distilled water were placed in 10 mm NMR tubes and heated in a water bath at  $96^\circ\text{C}$  for 5 h until fully dissolved and visually homogeneous. The samples were quenched immediately from  $96^\circ\text{C}$  to their designated storage temperature and were stored in a water bath at  $23$  or  $5^\circ\text{C}$  for varying periods of time. PEO was dissolved in water at room temperature by vortexing. All samples were capped to prevent water loss. PVA and PEO concentrations are reported as percent polymer by weight. Identification of a sample as a sol or a gel was done visually according to the method of Komatsu et al.<sup>22</sup> by observing the deformation of the meniscus under its own weight. All samples were equilibrated at  $23^\circ\text{C}$  for 15 min prior to analysis and returned to the temperature bath immediately following analysis.

**Instrumentation.** MT profiles of aqueous polymer samples were obtained from the offset-frequency dependence of the intensity of the water signal. The high-resolution spectra used to construct MT profiles were obtained on a Bruker AMX 360 wide-bore spectrometer operating at 360.13 MHz for the detection of protons. The spectrometer was equipped with a 25-mm single-frequency ( $^1\text{H}$ ) single-coil probe. The pulse sequence was D1 (relaxation delay)–P18 (preparation pulse)–P1 ( $90^\circ$  pulse)–acquisition. For all MT measurements, the preparation pulse was applied for 3 s at a radio-frequency field strength of 500 Hz (proton precessional frequency). The frequency offset ( $\Delta$ ) of the preparation pulse from the water resonance was varied from  $-70$  to  $+70$  kHz. Other acquisition parameters were a relaxation delay (D1) of 20 s, a  $90^\circ$  pulse (P1) of 56 ms, and a spectral width of 8196 Hz. All measurements consisted of a single scan and were carried out at  $23 \pm 2^\circ\text{C}$ . The typical time for measurement of an MT profile was 9 min.

Dynamic viscoelastic measurements were acquired with a stress-controlled rheometer (Rheometrics RDA II, Piscataway, NJ) using a 50 mm diameter parallel-plate geometry. The storage and loss moduli,  $G'(\omega)$  and  $G''(\omega)$ , of the samples were measured at a strain of 0.7% over an angular frequency range from 0.15 to 15 Hz at  $23^\circ\text{C}$  for 20% PVA samples of A–D. The sample rigidity is expressed in terms of the limiting value of the frequency-dependent storage modulus  $E = \lim_{\omega \rightarrow 0} G'(\omega)$  as  $\omega \rightarrow 0$  where  $\omega$  is the angular frequency and  $E$  is the relaxed shear modulus.<sup>23</sup> The gel rigidity is expressed as the limiting value of  $G'(\omega)$  at the lowest attainable experimental value of  $\omega$ , 0.15 Hz.

**Magnetization-Transfer NMR Spectroscopy.** Proton relaxation in a heterogeneous sample containing both liquid and solid components involves magnetic relaxation coupling between the components. This magnetic coupling may be exploited to examine the solid spin system, which is difficult to observe accurately, by means of the readily observed liquid component.<sup>24–26</sup> The MT experiment in this study was adapted from the work of Wu and Eads<sup>26</sup> from a technique described by Grad and co-workers<sup>24</sup> and has been successfully used to study naturally occurring macroscopically heterogeneous polymer systems.<sup>26–30</sup> Grad et al.<sup>24</sup> simplified the set of six coupled Bloch equations to describe a model system containing a pair of spin systems, A (mobile) and B (immobile), interacting via intermolecular dipole–dipole interactions in the rotating frame in the presence of a radio-frequency (RF) field. The observed magnetization ( $\bar{M}_A^S(t)$ ), which can be written in a reduced form

$$\bar{M}_A^S(t) = [M_A^0 - M_A^S(t)]/2M_A^0 \quad (1)$$

is a measure of the deviation of the longitudinal magnetization of the A spins from equilibrium at time ( $t$ ) in the absence of an RF field, where ( $M_A^S$ ) is the magnetization of the A signal in the presence of off-resonance saturation of the B spins and ( $M_A^0$ ) is the magnetization of the A signal in the absence of saturation.

The steady-state solution of the Bloch equations for a single population of nuclear spins is simplified in the following equation and contains the relaxation parameters of the immobile as well as of the mobile component. When the cross-relaxation rate between the mobile and immobile spins is much greater than unity, the measured liquid signal intensity ( $M_A^0(t)$ ) is affected by the magnetic relaxation parameters of the immobile spin system and, therefore, by the molecular dynamics of the immobile component.<sup>27</sup>

$$\bar{M}_A^S(t) = \frac{1}{2}[(\omega_1/T_{1B}T_{2B})/(1 + 4\pi^2T_{2B}^2\Delta^2)(1 + T_{1B}/fT_{1A}) + \omega_1 \times 2T_{1B}T_{2B})] \quad (2)$$

The quantity  $f$  refers to the ratio of the number of B spins to the number of A spins,  $\Delta$  represents the frequency offset of the preparation radio-frequency field from the A resonance frequency, and the quantities  $T_1$  and  $T_2$  are the spin–lattice and spin–spin relaxation times of the protons in the mobile (A) and immobile (B) components.<sup>24–26</sup>

Aqueous solutions and gels of PVA contain polymer-rich and solution-rich regions that we refer to as immobile and mobile components. The immobile component is defined as the polymer-rich portion of the sample that is characterized at a molecular level by restricted motion. The mobile component is defined as the solution-rich portion of the sample in which the polymer chains move freely. These freely moving chains become increasingly entangled and may ultimately form an immobile network as the system ages. In a system containing both mobile and immobile components, the slow-relaxing protons of the mobile component transfer magnetization to the fast-relaxing protons of the immobile component. The interaction between the immobile and mobile components of a gel is measured by saturating the proton NMR signal of the immobile component while avoiding any direct saturation of the proton signal from the mobile component. The intensity of the MT profile depends on the ratio ( $f$ ) of immobile protons to mobile protons. The area of the MT profile increases as the number of protons in the immobile component increases, and the line width of the MT profile increases with increasing rigidity of the system, i.e., decreasing spin–spin relaxation time of protons in the immobile component ( $T_{2B}$ ).

**Line-Shape Analysis.** The line shapes of the MT profiles were analyzed using simple line-shape functions in accordance with the procedure first described by Wu and Eads.<sup>26</sup> The MT profile is a plot of the normalized intensity of the water peak,  $M_A^S(\text{with presaturation})/M_A^0(\text{without presaturation})$ , versus the frequency offset  $\Delta$ . This plot must be inverted for curve-fitting analysis; thus, the function  $1 - M_A^S/M_A^0$  was used. The line shape was fit by a routine using a least-squares procedure (Sigma Plot, Jandel Scientific, Corte Madera, CA) to the sum of Lorentzian and Gaussian functions, and the intensities and full-width at half-maximum (fwhm) of the Gaussian and Lorentzian components were obtained from the curve-fitting analysis. The areas of the MT profile and its components were calculated as the sum of the values at intervals of 500 Hz over a frequency range of  $-70$  to  $+70$  kHz and were expressed in arbitrary units. The Gaussian percentage of the MT profile is defined as the area of the Gaussian component divided by the total area of the profile; the Lorentzian percentage of the MT profile is defined analogously. According to analyses in the literature, the total area of the MT profile may be used to a first approximation as an index of chain immobilization, but the area of the Gaussian component of the MT profile most specifically reflects the relative quantity of immobilized polymer chains in the sample, while the Lorentzian area represents the mobile portion of the sample.<sup>26,27, 31</sup>

## Results and Discussion

**Effect of Concentration and Degree of Hydrolysis on Network Formation.** Information from MT analyses was used to assess the influence of concentra-

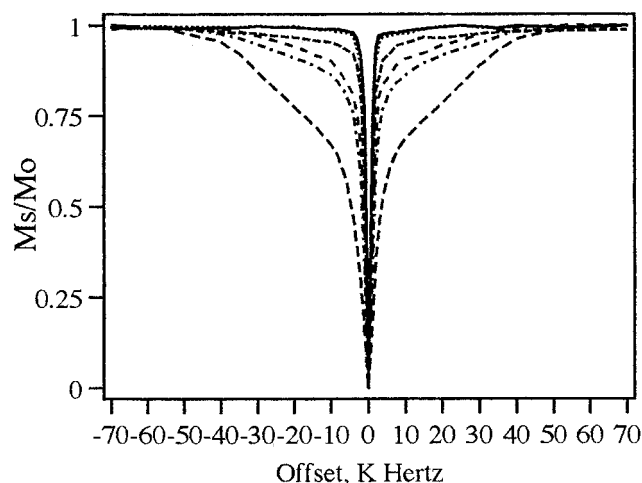


**Figure 1.** Magnetization-transfer profiles of PVA-A quenched and stored at 23 °C for 24 h (top to bottom): 5% (—), 10% (···), 12% (---), 17% (- · - ·), 20% (- - -), and 30% (- - -).

tion on the degree of network formation in aqueous solutions of PVA. The MT profiles as a function of the concentration of PVA-A (99.5% hydrolyzed) quenched and stored at 23 °C for 24 h are shown in Figure 1. As the concentration increases, the area of the MT profiles increases dramatically. The MT profiles of 5% and 10% PVA samples are narrow, characteristic of samples with a single mobile motional component with a single long transverse relaxation time ( $T_2$ ). At concentrations greater than 10%, the MT profiles are broad, indicating the existence of regions of restricted molecular motion characterized by shorter values of  $T_2$ . It is likely that several  $T_2$  values characterize subdomains of varying mobility within this generally immobile portion of the sample.

The area of the MT profile increases nonlinearly with increasing polymer concentration for all PVA samples with varying degrees of hydrolysis stored for 1 day at 23 °C (Figure 2a). The nonlinear increase in the profile area again indicates more extensive network formation at higher PVA concentrations. However, a greater deviation from linearity is evident as the degree of hydrolysis of the polymer increases. These data suggest increasing polymer–polymer hydrogen bonding, likely at the expense of polymer–solvent associations, as the degree of hydrolysis increases and hence as the number of residual acetate groups on the polymer backbone decreases.

In polymer systems, changes in molecular mobility with increasing polymer concentration also result from increases in solution viscosity and gel viscoelasticity. To confirm that MT analysis is reporting network formation and not simply changes in viscosity, solutions of poly(ethylene oxide) (PEO), a water-soluble polymer that does not contain pendant groups capable of hydrogen bonding, were analyzed by MT in the 5–40% concentration range. The viscosities of these solutions are comparable to those of the PVA solutions studied. The MT profiles of PEO samples were fit to a single narrow Lorentzian function ( $\text{fwhm} < 2$  kHz) and did not increase with increasing polymer concentration (Figure 2b). Because the MT profiles of the PEO solutions do not broaden as viscosity increases, the change in profile area of the PVA solutions and gels may be ascribed with confidence to chain immobilization resulting from polymer–polymer self-association and consequent network formation.

The MT profiles of 5, 10, 15, 20, and 30% samples of PVA-A, -B, -C, and -D were acquired after the samples were quenched and stored at 23 °C for 24 h. The area of each profile was calculated and plotted as a function of the degree of hydrolysis (Figure 3). After 1 day of storage at 23 °C, the degree of network formation is negligible in 5% PVA samples at all degrees of hydrolysis as indicated by narrow MT profiles. The onset of chain overlap and entanglement has been reported to occur in aqueous solutions of PVA with a  $\text{dp}$  of 1700 and a concentration of polymer from 2 to 4 wt %. It is highly likely that the 5% solutions of PVA ( $\text{dp}$  1250–1300) studied herein are below the critical concentration at which entanglement takes place. Of course, it is also possible that the degree of network formation in these samples after 1 day of storage is simply below the detection limits of MT analysis.

In the PVA-D sample, network formation is minimal at all concentrations as indicated by very low profile areas. The PVA-D sample contains 12.4% residual vinyl acetate that apparently corresponds to sufficient, bulky hydrophobic acetate groups to disrupt polymer–polymer inter- and intrachain hydrogen bonds and to favor polymer–solvent interactions. In the PVA-A, PVA-B, and PVA-C samples containing 0.5%, 1.5%, and 2.6% vinyl acetate, respectively, network formation is indicated by profile areas that increase in the order of decreasing residual vinyl acetate ( $\text{PVA-C} < \text{PVA-B} < \text{PVA-A}$ ), implying that polymer–polymer hydrogen bonding becomes increasingly dominant in the system as the percent hydrolysis increases. The critical concentration of acetate groups necessary to disrupt polymer–polymer hydrogen bonding is in the range of 3%, as the differences between PVA-D (12.4%) and PVA-C (2.6%) are small but real while the differences among PVA-C, PVA-B, and PVA-A are considerable, especially at concentrations above 15%.

**Aging of PVA.** For aqueous PVA gels, the development of a physically entangled network proceeds over many weeks in a process that can be monitored by observing changes in the MT profiles as the gels age. Figure 4 shows profiles as a function of time for 30% PVA-A (part a) and 30% PVA-D (part b) as samples age at 23 °C over an 18-week period. The MT profiles of PVA-A broaden and significantly increase in area with storage time. After only 1 day of storage, the breadth of the profile indicates considerable chain immobilization which continues to increase over time. In contrast, the MT profiles of PVA-D do not broaden or increase greatly in area over the 18-week period, indicating negligible network formation. PVA-A with 0.5% residual acetate groups experiences more extensive polymer–polymer inter- and intrachain hydrogen bonding and hence network formation than PVA-D, with 12.4% residual acetate, for which polymer–solvent interactions predominate and network formation is minimal.

The evolution of network formation in 20% PVA samples with varying degrees of hydrolysis was monitored as a function of storage time at 23 and 5 °C (Figure 5a and b and Tables 1 and 2). The initial profile areas of all samples quenched and stored at 5 °C are larger for polymers of a given degree of hydrolysis than those quenched and stored at 23 °C. This is a direct consequence of the fast quench from the dissolution temperature of 96 °C to the storage temperature of 5 °C. The lower quench temperature promotes network formation that results in extensive chain immobilization as indicated by the broad initial MT profiles.

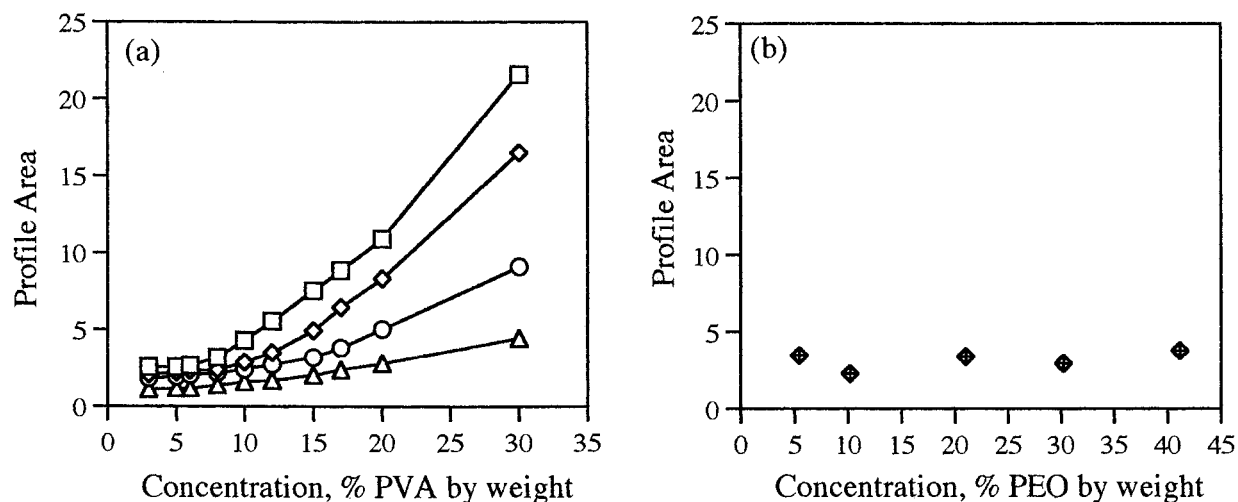


**Figure 2.** (a) Profile area measured as a function of PVA concentration for samples A ( $\square$ ), B ( $\diamond$ ), C ( $\circ$ ), and D ( $\triangle$ ) stored at 23 °C for 24 h. (b) Profile area measured as a function of PEO concentration stored at 23 °C for 24 h.

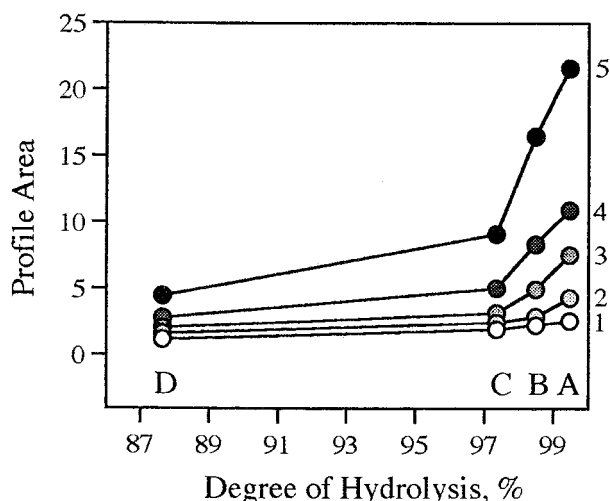


**Figure 3.** Profile area measured as a function of the degree of hydrolysis for 5% (1), 10% (2), 15% (3), 20% (4), and 30% (5) samples of PVA stored at 23 °C for 1 day.

After 18 weeks, PVA-A stored at 23 °C shows a more extensive network than PVA-A stored at 5 °C, as indicated by a significantly larger profile area. The lower storage temperature hinders continued development beyond the initial network in PVA-A. In contrast, PVA-B and PVA-C develop a more extensive network over time at 5 °C than at 23 °C. The area of the profile of PVA-B at 5 °C approaches that of PVA-A ( $A \sim B > C > D$ ), whereas at 23 °C the areas of A, B, and C are widely separated, but  $C \sim D$  ( $A > B > C \sim D$ ). The sensitivity to temperature of the differences between A and B on the one hand and C and D on the other hand—that  $A \sim B$  and  $C > D$  at 5 °C but  $A > B$  and  $C \sim D$  at 23 °C—suggests that at low temperature the samples demonstrate the maximum amount of network formation that the polymer can achieve based on the competition between thermal motion of the chains and polymer–polymer hydrogen bonding to produce the network; hence, discrimination is sharpest between network formers as a group (A, B, and C) and the nonnetwork former (D). (This trend is even more pronounced at a concentration of 30%, where at 5 °C  $A \sim B \sim C > D$ ; data are not shown.) At the higher temperature we observe that motion of the chains and polymer–solvent interactions compete successfully with polymer–polymer interactions, so the discrimination is

sharpest among those samples in which slight variations in the number of residual acetate groups impact the extent of polymer–polymer vs polymer–solvent interaction ( $A > B > C$ ), with C being close to D in terms of the minimum number of residual acetates necessary to tip the balance. The behavior of C relative to D supports the view that as little as 3% residual acetate concentration is sufficient to shift the balance between polymer–solvent and polymer–polymer interactions in determining properties of the aqueous mixtures at room temperature.

In addition, the PVA samples stored for 18 weeks at 23 °C are visually different from than the corresponding samples stored at 5 °C. All four samples at 5 °C and the PVA-D sample at 23 °C are transparent, while the PVA-A, -B, and -C samples stored at 23 °C are opaque. This opacity indicates that the PVA-A, -B, and -C samples stored at 23 °C become phase separated. To modify our picture of interactions to accommodate this observation, we evaluated changes in the Gaussian and Lorentzian components of the profile in addition to the overall profile area.

**Multicomponent Nature of MT Profiles.** Additional information at the molecular level on the effect of the degree of hydrolysis and temperature on network formation may be gleaned from the Gaussian and Lorentzian components of the MT profiles.<sup>26,27</sup> In general, the spectral line shape of a sample with a single motional component with a characteristic  $T_2$  is described by a Lorentzian function.<sup>24–26</sup> The MT profiles of aged PVA samples cannot be described by a single Lorentzian function, because they contain an additional component with a short  $T_2$  due to immobilized polymer. These complex MT profiles were fit to a function that is the sum of a narrow Lorentzian component and a broad Gaussian component (Figure 6). The mobile component is the portion of the system containing both polymer and water that gives rise to the Lorentzian line shape, while the immobile component is the portion of the system containing both polymer and water with collectively restricted motion that gives rise to a Gaussian line shape.

Wu and Eads reported that the fwhm of the Gaussian components of MT profiles corresponded closely to the rigidity of starch gels.<sup>26</sup> To test the validity of extending this relationship to the Gaussian area of PVA gels, the rigidity of the samples was measured by dynamic

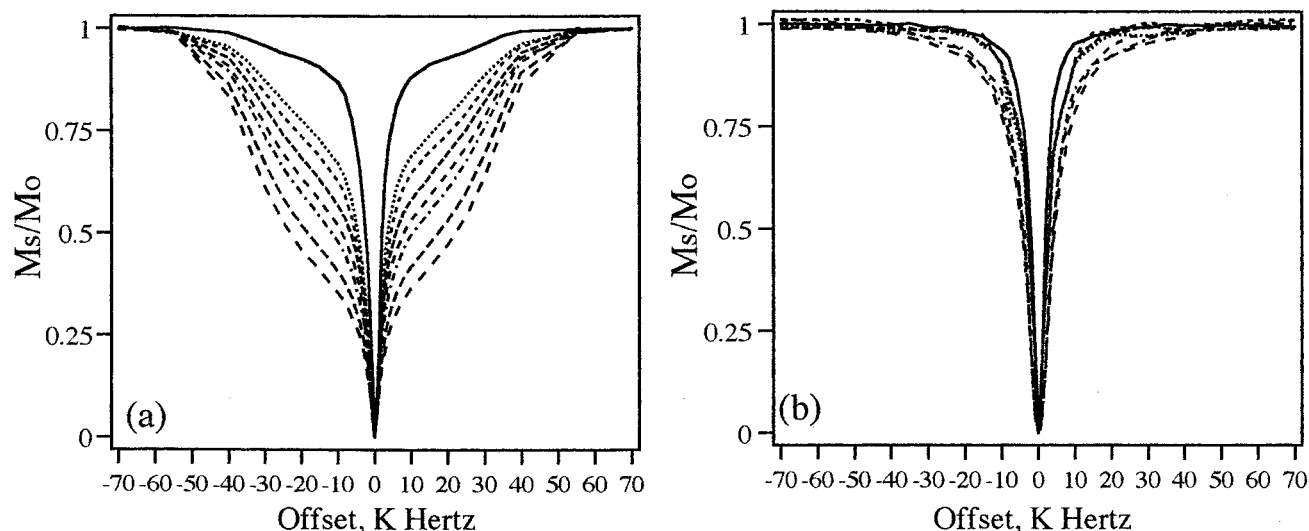


**Figure 4.** MT profiles of (a) 30% PVA-A and (b) 30% PVA-D stored at 23 °C for (top to bottom) 15 min (—), 1 day (---), 3 days (---), 8 days (---), 14 days (---), 21 days (---), 49 days (---), and 126 days (---).

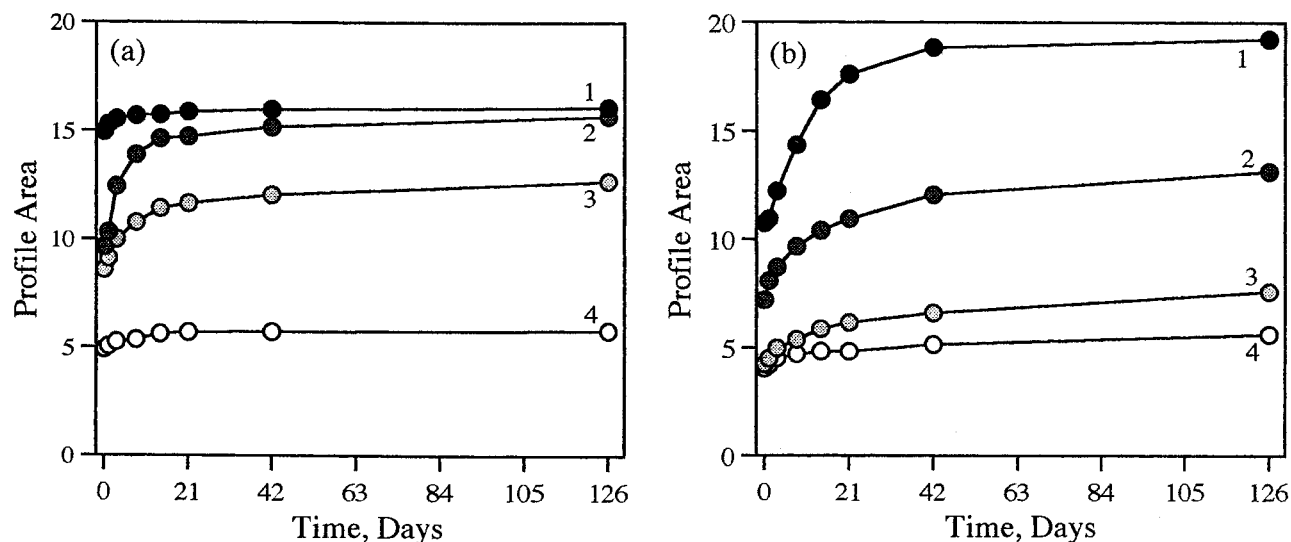


**Figure 5.** MT profile area as a function of storage time (a) 5 °C and (b) 23 °C for 20% PVA (1), PVA-B (2), PVA-C (3), and PVA-D (4).

**Table 1. Line-Shape Analysis of 20% PVA-A, PVA-B, and PVA-C Stored at 23 °C**

storage time, days	PVA-A				PVA-B				PVA-C			
	profile area	Gaussian area	Lorentzian area	G/L	profile area	Gaussian area	Lorentzian area	G/L	profile area	Gaussian area	Lorentzian area	G/L
0	10.7	5.5	5.2	1.1	7.2	1.3	5.9	0.2	4.2	0.0	4.2	
1	11.0	6.8	4.2	1.6	8.1	3.7	4.4	0.8	4.5	0.0	4.5	
3	12.2	8.6	3.6	2.4	8.7	4.8	3.9	1.2	5.0	1.1	3.9	0.3
7	14.9	10.9	4.0	2.7	9.7	7.1	2.6	2.7	5.4	1.3	4.1	0.3
14	16.4	12.8	3.6	3.6	10.4	7.7	2.7	2.9	5.9	1.4	4.5	0.3
21	17.6	14.1	3.5	4.0	10.9	7.9	3.0	2.6	6.2	1.6	4.6	0.3
42	18.9	15.7	3.2	4.9	12.0	8.6	3.4	2.5	6.6	1.8	4.8	0.4
126	20.0	16.3	3.7	4.4	13.1	9.5	3.6	2.6	7.6	1.9	5.5	0.3

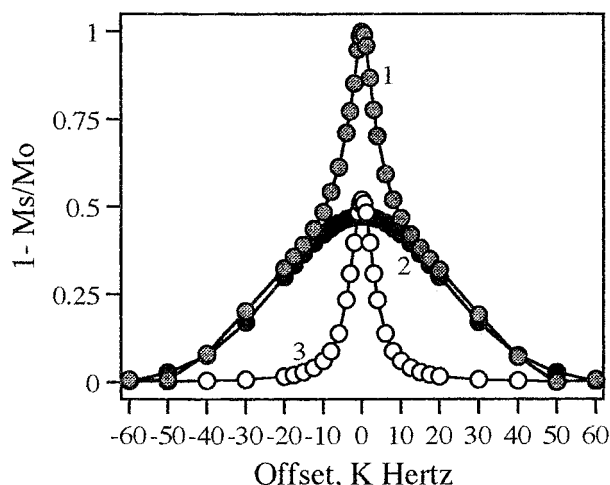
mechanical testing (Figure 7a and b). Gel rigidity was determined for 20% samples of PVA-A, -B, -C, and -D stored at 23 °C for 3 days. The measured rigidity is expressed as the limiting value of the frequency-dependent storage modulus and is plotted as a function of the degree of hydrolysis in Figure 7b. The gel rigidity measured by this method follows the same trend as the Gaussian area of the MT profiles with increasing degree of hydrolysis (Figure 7a). The Gaussian area of the gel thus yields an estimation of the relative rigidity of the gel without mechanically disrupting or destroying the gel.

The MT profiles over time of 20% samples of PVA-A, -B, and -C stored at 5 °C (Table 1) and 23 °C (Table 2) were fit to a function that is the sum of a broad Gaussian component and a narrow Lorentzian component. Analysis of these two components provides insight regarding the balance between the polymer-rich and solution-rich portions of the samples. As the samples age, the total profile areas and Gaussian areas of 20% samples of PVA-A, -B, and -C increase.

The total profile area and Gaussian area are largest for the sample with the highest degree of hydrolysis, PVA-A. When this sample at the initial time point is

**Table 2.** Line-Shape Analysis of 20% PVA-A, PVA-B, and PVA-C Stored at 5 °C

storage time, days	PVA-A				PVA-B				PVA-C			
	profile area	Gaussian area	Lorentzian area	G/L	profile area	Gaussian area	Lorentzian area	G/L	profile area	Gaussian area	Lorentzian area	G/L
0	15.0	10.5	4.5	2.3	9.6	4.8	4.8	1.0	8.6	3.9	4.7	0.8
1	15.3	11.2	4.1	2.7	10.3	5.0	5.3	0.9	9.1	4.9	4.2	1.2
3	15.6	11.5	4.1	2.8	12.4	7.8	4.6	1.7	10.0	5.5	4.4	1.2
7	15.7	11.7	4.0	2.9	13.9	10.1	3.9	2.6	10.8	5.7	5.1	1.1
14	15.7	11.8	3.9	3.0	14.6	10.8	3.8	2.8	11.4	5.7	5.5	1.1
21	15.9	12.0	3.9	3.1	14.7	11.0	3.7	3.0	11.7	6.0	5.7	1.1
42	16.0	12.1	3.9	3.1	15.2	11.4	3.8	3.0	12.1	6.1	6.0	1.0
126	16.1	12.2	3.9	3.1	15.7	11.6	4.1	2.8	12.0	6.1	5.9	1.0

**Figure 6.** Curve-fitting analysis of the magnetization-transfer profile for a 30% sample of A stored for 24 h at 23 °C. Actual profile area (1), Lorentzian (3), and Gaussian curve (2).

tilted at a 90° angle, its meniscus does not deform; the sample is a gel.<sup>22</sup> The initial profile of this sample stored at 23 °C is 51% Gaussian.

When the 20% PVA-B sample stored at 23 °C is tilted at 90° at the initial time point, the sample deforms; it is a solution.<sup>22</sup> The area of the MT profile of this sample is only 18% Gaussian. After storage for 18 weeks at 23 °C, the meniscus of the sample does not deform when tilted, and its MT profile is 72% Gaussian; the material has become a gel.

The MT profile of a 20% sample of PVA-C quenched at 23 °C does not contain a Gaussian component, and a Gaussian component is not detected in the system for 3 days; prior to 3 days of storage the entanglements of the chains have simply not developed sufficiently to be detected as a network. The MT profile of the sample at 3 days of storage is 22% Gaussian and remains below 50% for the entire storage period. When the sample is tilted after 18 weeks, the meniscus deforms; the sample is a solution over the entire storage period.

On the basis of behavior of the samples studied, a sample with an MT profile that is 50% Gaussian or greater is more solidlike than liquidlike. As a result such a sample may be considered a gel from the point of view of NMR.

The Lorentzian areas decrease with storage time for samples PVA-A and -B stored at 23 °C. The decrease in the Lorentzian area is the direct result of a decrease in the line width of the Lorentzian component, which in turn suggests an increase in the mobility of the chains in this portion of the system. An increase in the mobility of the chains in the mobile fraction can occur if the loosely entangled chains of the Gaussian component become increasingly immobilized and tighten,

thereby decreasing the volume they occupy. A decrease in the volume of the Gaussian component results in an increase in the volume available for the mobile chains, thereby effectively diluting the chains and increasing their mobility. This interpretation suggests a possible reason for the observed opacity of the samples stored at 23 °C: tightening the chains in the immobile fraction and diluting the remaining mobile chains would produce increasingly polymer-rich and solution-rich regions that ultimately progress to separated phases and hence opaque samples.

Relative changes in the Gaussian and Lorentzian components within a given sample and among several samples enable us to sharpen the picture at the molecular level of network formation and phase separation in PVA solutions and gels. The Gaussian areas of the samples stored at 5 °C increase with the age of the samples and are the largest for the samples with the highest degrees of hydrolysis. The initial MT profile of a 20% PVA-A sample stored at 5 °C is 70% Gaussian. This sample, a gel, is more rigid than the corresponding sample stored at 23 °C, whose initial MT profile is only 51% Gaussian. After 18 weeks at 5 °C, the MT profile of the 20% PVA-A sample is 76% Gaussian, a net increase of only 6%. The profile of the corresponding sample at 23 °C is 82% Gaussian, a net increase of 31%. As previously suggested, the initial 5 °C quench promotes rapid chain organization, but the lower storage temperature restricts further progression of the network. In the PVA-A sample quenched and stored at 23 °C, less initial network formation takes place, but the thermal energy available is sufficient to promote the continuing development of the network by chains that sample alternative configurations in their progress to localized energy minima.

The MT profile of the 20% PVA-B sample quenched at 5 °C is 50% Gaussian and rises to 74% after 18 weeks at 5 °C. The MT profile of the corresponding sample quenched and stored at 23 °C is only 18% Gaussian initially and rises to 72% after 18 weeks. The maximum Gaussian percentage in the samples is achieved within 7 days of storage at either temperature. For PVA-B, the 5 °C quench appears to promote initial chain organization as it did with sample PVA-A. In PVA-B, however, the temperature does not restrict further progression of the network as much, probably in part due to the slightly more prominent polymer-solvent interactions because of the lower degree of hydrolysis.

The MT profile of the 20% sample of PVA-C quenched and stored at 5 °C is 45% Gaussian and rises to 51% after 18 weeks. Most network formation in this sample is due to initial chain organization as a result of the low-temperature quench. The MT profile of the corresponding PVA-C sample at 23 °C does not contain an initial Gaussian component; a 22% Gaussian component

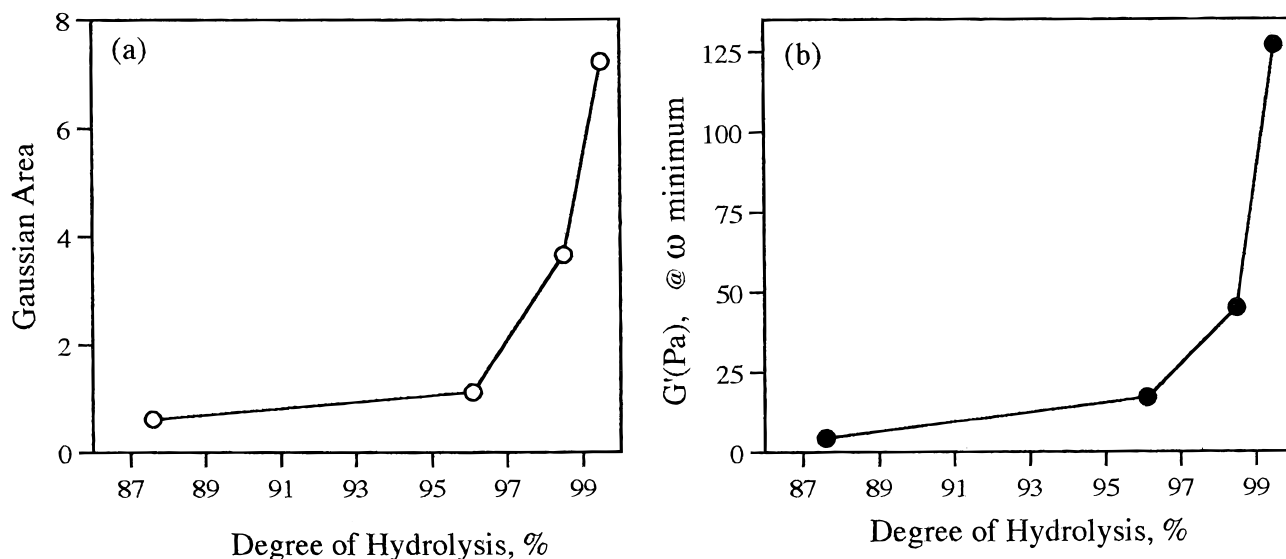


**Figure 7.** (a) Gaussian area of the MT profiles measured for 20% PVA samples stored at 23 °C for 3 days. (b) Gel rigidity measured at 23 °C for 20% PVA samples stored at 23 °C for 3 days.

develops only after 3 days of storage. At 23 °C the chains are extremely mobile and interact even more extensively with solvent; this behavior decreases the extent to which network forms. After 18 weeks at 23 °C, the MT profile of the corresponding PVA-C sample is only 25% Gaussian.

### Conclusions

Network formation in all PVA samples studied increases nonlinearly with concentration over 1 day, and the higher the concentration of polymer, the more extensive the network formation. In the PVA sample containing 12.4% residual vinyl acetate, polymer-solvent interactions are favored as evidenced by the negligible formation of network at high concentrations and long times. The critical concentration of acetate groups required to disrupt the inter- and intrachain hydrogen bonding responsible for the formation of the network is in the range of 3%. All samples quenched and stored at 5 °C demonstrate more extensive initial network formation than those at 23 °C; however, after 18 weeks, differences may be noted in the extent of the network evolved over time for the polymers as a function of the degree of hydrolysis. At the higher temperature, differences are greatest among samples with the highest degree of hydrolysis, perhaps indicating sensitivity at that temperature to small changes in the number of residual acetate groups impacting the competition between polymer-polymer and polymer-solvent interactions. At the lower storage temperature, network formation is maximized for the polymers, so discrimination is sharpest between those samples that form networks and those that do not.

Relative changes in the areas of the Gaussian and Lorentzian components of the samples over time suggest that the networks in samples stored at 23 °C change in a fashion different from those at 5 °C. At the higher temperature, the samples become opaque and phase separate as the immobile component tightens over time. At the lower temperature, extensive further development of the initially established organization is restricted; more network forms but existing network does not tighten and hence phase separation does not occur.

**Acknowledgment.** The authors thank Dr. Mary Jo Kulp of Air Products and Chemicals, Inc., for the PVA

samples and the helpful discussions and William R. Anderson, Jr., and Dr. D. J. Wang of Lehigh University for their assistance with the NMR experiments.

### References and Notes

- (1) *Poly(Vinyl Alcohol): Developments*; Finch, C. A., Ed.; John Wiley: London, 1992.
- (2) Toyoshima, K. In *Poly(Vinyl Alcohol), Properties and Applications*; Finch, C. A., Ed.; John Wiley: London, 1973.
- (3) *Poly(Vinyl Alcohol), Basic Properties and Uses*; Pritchard, L. G., Ed.; Gordon and Breach: London, 1970.
- (4) Sakurada, I. *Poly(Vinyl Alcohol) Fibers*; Marcel Dekker: New York, 1985.
- (5) Komatsu, M.; Inoue, T.; Miyasaka, K. *J Polym. Sci., Polym. Phys. Ed.* **1986**, *24*, 303–311.
- (6) Wu, W.; Shibayama, M.; Roy, S.; Kurokawa, H.; Coyne, L.; Nomura, S.; Stein, R. S. *Macromolecules* **1990**, *23*, 2245–2251.
- (7) Kanaya, T.; Ohkura, M.; Takeshita, H.; Kaji, K.; Furshaka, M.; Yamamoka, H.; Wignall, G. D. *Macromolecules* **1995**, *28*, 3168–3174.
- (8) Kobayashi, M.; Ando, I.; Ishii, T.; Amiya, S. *Macromolecules* **1995**, *28*, 6677–6679.
- (9) *Properties of Polymers: Their Correlation with Chemical Structure*, 3rd ed.; Van Krevelen, D. W., Ed.; Elsevier: New York, 1990.
- (10) Ohkura, M.; Kanaya, T.; Kaji, K. *Polymer* **1992**, *33*, 5044–5047.
- (11) Matsuo, M.; Kawase, M.; Sugiura, Y.; Takematsu, S.; Hara, C. *Macromolecules* **1993**, *26*, 4461–4471.
- (12) Matsuzawa, S.; Yamaura, K.; Kobayashi, H. *Colloid Polym. Sci.* **1981**, *259*, 1147–1150.
- (13) Nagura, M.; Hamano, T.; Ikhikawa, H. *Polymer* **1989**, *30*, 762–765.
- (14) Fang, L.; Brown, W. *Macromolecules* **1990**, *23*, 3284–3290.
- (15) Horkay, F.; Burchard, W.; Geissler, R.; Hecht, A. M. *Macromolecules* **1993**, *26*, 1296–1303.
- (16) Stern, P.; Prokopova, E.; Quadrat, O. *Colloid Polym. Sci.* **1985**, *263*, 899–904. Stern, P.; Prokopova, E.; Quadrat, O. *Colloid Polym. Sci.* **1987**, *265*, 234–238. Prokopova, E.; Stern, P.; Quadrat, O. *Colloid Polym. Sci.* **1987**, *265*, 903–907. Mrkvickova, L.; Prokopova, E.; Quadrat, O. *Colloid Polym. Sci.* **1987**, *265*, 978–981. Stern, P.; Prokopova, E.; Quadrat, O. *Colloid Polym. Sci.* **1992**, *270*, 1066–1068.
- (17) Yokayama, F.; Masada, I.; Shimamura, K.; Ikawa, T.; Monobe, K. *Colloid Polym. Sci.* **1986**, *264*, 595–601.
- (18) Prokopova, E.; Biros, J.; Lednický, F. *Eur. Polym. J.* **1988**, *24*, 621–664.
- (19) Cha, W.-I.; Hyon, S.-H.; Ikada, Y. *Makromol. Chem.* **1983**, *194*, 2433–2441.
- (20) Hatakeyema, T.; Jamauchi, F. *Eur. Polym. J.* **1984**, *20*, 61–64. Hatakeyema, T.; Jamauchi, F.; Hatakeyema, H. *Eur. Polym. J.* **1987**, *23*, 361–365.

- (21) Urayama, K.; Takigawa, T.; Masuda, T. *Macromolecules* **1993**, *26*, 3092–3096.
- (22) Komatsu, M.; Inour, T.; Miyasaka, K. *J. Polym. Sci., Polym. Phys. Ed.* **1986**, *24*, 303–311.
- (23) Almdal, K.; Dyre, J.; Hvidt, S.; Kramer, O. *Polym. Gels Networks* **1993**, *1*, 5–17. Hvidt, S.; Heller, K. In *Physical Networks, Polymers and Gels*; Burchard, W., Ross-Murphy, R. B., Eds.; Elsevier Applied Science: New York, 1990; Chapter 16. Djabourv, M. *Polym. Int.* **1991**, *25*, 135–143.
- (24) Grad, J.; Mendelson, D.; Hyder, F.; Bryant, R. G. *J. Magn. Reson.* **1990**, *86*, 416–452.
- (25) Grad, J.; Bryant, R. G. *J. Magn. Reson.* **1990**, *90*, 1–8.
- (26) Wu, J. Y.; Eads, T. M. *Carbohydr. Polym.* **1993**, *20*, 51–60.
- (27) Ni, Q. X.; Eads, T. M. *J. Agric. Food Chem.* **1993**, *41*, 1035–1040.
- (28) Wolff, J. Y.; Balaban, R. S. *Magn. Reson. Med.* **1989**, *10*, 135–144.
- (29) Edzes, H. T.; Samulski, E. T. *J. Magn. Reson.* **1978**, *31*, 207–229.
- (30) Konig, S. H.; Brown, R. D. *Magn. Reson. Med.* **1993**, *30*, 685–695.
- (31) Kennan, R. P.; Richardson, K. A.; Zhong, J.; Maryanski, M. J.; Gore, J. C. *Magn. Reson., Ser. B* **1996**, *110*, 267–277.

MA971425H